University of Baghdad
College of Engineering
JE
JOURNAL OF ENGINEERING

Journal of Engineering
journal homepage: www.jcoeng.edu.iq
Volume 31 Number 1 January 2025

Effect of Perlite Aggregate Replacement of Coarse Aggregate on the Behavior of SCC Exposed to Fire Flame by Using Different Cooling Methods

Baraa Qays Naeem*, Hadeel Khaled Awad

Department of Civil Engineering, College of Engineering, University of Baghdad, Baghdad, Iraq

ABSTRACT

The qualities of both fresh and hardened perlite self-compacting concrete are assessed in this study. The self-compacting concrete mix utilized in this investigation included 594 kg/m^3 of binder. Four concrete mixes were tested with perlite used in place of some of the coarse aggregate at volumetric ratios of (0, 20, 40, and 50) %. Slump flow, V-funnel, L-Box, and segregation index tests were used to evaluate the properties of fresh concrete. At 56 days after burning, hardened concrete is tested. These tests gauge a material's flexural, splitting, and compressive strengths. According to the data perlite content reduces workability. The percentage of perlite increases causes a considerable decrease in the compressive, flexural, and splitting tensile strengths when compared to the reference mixture. Following their burning at (300, 500, and 700 °C), half of the specimens cooled gradually before being tested, while the other half cooled rapidly. The residual percentages of Compressive strength at 56 days after burning were the most at 50% perlite, with (89.75,65.21, and 42.86) % at 300, 500, and 700 C°, respectively for gradual cooling. The residual percentages of Splitting tensile strength at 56 days after burning for PG50% were (98.85,85.22and 51.31) % at 300, 500, and 700 C°, respectively for gradual cooling.

Keywords: Coarse aggregate, Fire flame, Perlite aggregate, Self-compacting concrete.

1. INTRODUCTION

SCC was created in the middle of the 1980s. It has a unique ability to fill molds and flow this form of concrete doesn't require external vibration **(Al-Kabi and Al-Obaidy, 2024).** Due to its special properties, SCC has the potential to significantly increase the performance of concrete structures and increase the variety of applications for concrete **(Alsaedy and Aljalawi, 2012).** The attributes within the concrete are significantly impacted by the chrematistics of the materials. The high density of SCC mixes increases structure weight,

*Corresponding author
Peer review under the responsibility of University of Baghdad.
https://doi.org/10.31026/j.eng.2025.01.04
This is an open access article under the CC BY 4 license (http://creativecommons.org/licenses/by/4.0/).
Article received: 24/04/2024
Article revised: 16/09/2024
Article accepted: 10/10/2024
Article published: 01/01/2025

which has led to an increase in the cost of construction. the drawback cause mitigated by using lightweight aggregates instead of standard coarse aggregates **(Shamran and Abbas,2022).** ACI 237R-14 defines self-compacting concrete (SCC) as strongly flowing concrete that can permeate and separate from the reinforcing without the necessity for compaction or mechanical consolidation

SCC can be distributed by filling the structure's framework **(Aljalawi and Ahmed, 2014; Al-Obaidy, 2017)**. To meet its stated workability standards, SCC must possess the following three qualities: filling ability, passing ability, and segregation resistance **(EFNARC, 2002)**. Self-compacting concretes, which depend upon their own weight for flow, have less internal energy and flow a little bit more slowly when lightweight aggregate is employed than natural aggregate concretes **(Hubertova, 2005)**. An amorphous igneous rock with an aluminum-siliceous composition, perlite is created when volcanic lava crystallizes. Among its many physical attributes are its great spall resistance, fire and heat resistance, and good acoustic qualities. Its exceptional qualities as a thermal insulator have contributed to the development of concrete technology **(Premalatha et al., 2023; Al-Kabi and Al-Obaidy, 2024)**. When perlite gets heated to 870–1200 ˚C, it can expand to a size that is 15–35 times larger than its original volume. Due to its 2-5% water content, it transforms into a flexible, bulk-density material that is full of holes. Perlite is identified under a microscope by its thick and thin laminar sheets **(Cojocaru, 2023; Al-Daraji and Aljalawi, 2024)**. the density of perlite reaches 400 kg/m^3, which is not excessive in contrast to the density of many other minerals. Perlite has a specific gravity of 2.2 to 2.4 and a pH range of 6.5-8 **(Rashad, 2016)**. Because of its special qualities, perlite is a rare and adaptable mineral that is employed in many different industrial applications. With a low density, perlite's foamy-like microstructure is one of its most remarkable features. Its low density combined with its high porosity and outstanding thermal insulation qualities makes it the perfect option for a lightweight mineral filler in a different use **(Sodeyama,1999; Mladenovič et al., 2004).** To remedy the lack of qualified concrete workers and the drawbacks of conventional concrete in overcrowded situations, Prof. Okamura founded SCC in Japan in 1986. **(Aslani and Kelin, 2018)**. Many studies have been conducted on the using perlite aggregates in construction material techniques, particularly the effects of expanded perlite on the characteristics of concrete. According to these researches, using perlite in concrete mixes can enhance its weight and thermal insulation **(Sengul et al., 2011)**. **(Türkmen and Kantarcı, 2007)** found that added perlite (0–4) mm, substituted for a portion of natural sand at volumetric rates of (5, 10, and 15%), decreased the fresh unit weight by 0.74%, 0.91%, and 0.95%, respectively. The present results agree with previous studies that observed a linear reduction in the initial weight of concrete mixtures containing perlite at concentrations between 5 and 100%**. (Oktay et al.,2015)** discovered that using perlite in a mixture of concrete replaced of portion of sand reduced heat conductivity. According to the study, adding 10%, 20%, 30%, 40%, and 50% volume of EP particles with a variety of sizes of(0.15–11) mm to natural sand lowered the thermal conductivity of the concretes at 28 days by (22.96, 38.01, 64.23, 74.36, and 81.48%, respectively). **(Jedidi et al., 2015)** discovered that utilizing different Perlite particle sizes—ranging from 2 mm to 4 mm—in replacement of natural sand in a largely volumetric replacement with varied percentages (15, 30, 45, and 60) can lower heat conductivity by as much as 9.68%, 17.74%, 43.55%, and 66.13%, respectively.

(Gandage et al., 2013) Investigated thermal conductivity using perlite in three different percentages (2.5, 5, and 7.5%) and fly ash in M-40 SCC grade. The samples' bending strength

was determined to be 4.5 MPa after 28 days. After 28 days, the samples' maximum compressive strength was 51.852 MPa, with 5% perlite being the optimal range.
This study aims to investigate the impact of using perlite aggregate in place of coarse particle behaviour of self-compacting concrete exposed to fire.

2. RAW MATERIAL AND METHOD

2.1 RAW Materials

2.1.1 Ordinary Portland Cement

Ordinary Portland Cement (OPC) (CEM I-42.5 R) was used to prepare all concrete mixes. The chemical and physical characteristics of OPC are displayed in **Tables 1 and 2**. The results demonstrate that the OPC satisfies Iraqi regulations **(IQS No. 5, 2019).**

Table 1. Chemical properties of OPC.

Chemical composition	**Result**	**(IQS No.5, 2019)**
Lime (CaO)	64.8	----
Silica (SiO_2)	22.57	----
Alumina (Al_2O_3)	5	----
Iron Oxide (Fe_2O_3)	4.32	----
Magnesia (MgO)	3.1	5.0 max
Sulfate (SO_3)	2.22	≤ 2.8 If $C_3A > 3.5$
Insoluble residue (I.R)	0.84	1.5 max
Loss of ignition (L.O.I)	2	4 max
OPC Compounds		
Tri calcium silicate (C_3S)	52	---------
Di calcium silicate (C_2S)	20.74	---------
Tri calcium aluminate (C_3A)	9.12	---------
Tetra calcium aluminate ferrite (C_4AF)	10.10	---------

Table 2. The physical properties of ordinary Portland cement.

Properties	**Results**	**(IQS No.5, 2019)**
S.S.A m^2/kg (Blaine method)	381	≥ 280
Initial setting, (min)	165	≥ 45
The final setting, (hr: min)	4:30	≤ 10
Compressive strength, (MPa): at 2 days	23	≥ 20
at 28 days	44	≥ 42.5

2.1.2 Fine Aggregate (Sand)

The findings of using natural sand revealed that its grading and qualities complied with **(IQS No. 45, 1984)**. **Table 3** displays the sand grade that was found to be in Zone 2. **Table 4** presents the chemical and physical properties of sand.

Table 3. The grade of sand.

Sieve size (mm)	Passing %	Limit of (IQS No.45, 1984), zone 2
10	100	100
4.75	92.5	90-100
2.36	80	75-100
1.18	70	55-90
0.6	54	35-59
0.3	25	8-30
0.15	5	0-10
Fineness Modulus	2.735	

Table 4. The chemical and physical properties of fine aggregate**.**

Property	Specification	Result	Limits of (IQS No.45,1984)
Specific gravity	**(ASTM C128, 2007)**	2.58	--------
Absorption %	**(ASTM C128, 2007)**	0.94	--------
Dry rodded density (kg/m^3)	**(ASTM C29, 2007)**	1647	--------
Sulfate content % (SO_3)	**(Iraqi Reference Guide No. 500, 1994)**	0.26	0.5%(max)
Fine particles passing from the sieve 75 µm, %	**(Iraqi Reference Guide No. 500, 1994)**	2.73	5.0%(max)

2.1.3 Coarse Aggregate

Every concrete mixture contained a single size of 10 mm gravel. Iraqi criteria **(IQS No.45, 1984)** for the grading of coarse aggregate. **Table 5** shows the course aggregate grading, while **Table 6** presents the chemical and physical parameters of coarse aggregate.

Table 5. Grading of Coarse aggregate.

Sieve size (mm)	Passing %	Limit of (IQS No.45, 1984) max size 10 mm
20	100	100
14	100	100
10	92.5	85-100
5	18	0-25
2.36	5	0-5

Table 6. Chemical and physical characteristics of coarse aggregate (gravel).

Property	Specification	Test result	Limits of (IQS No. 45, 1984)
Specific gravity	**(ASTM C128, 2007)**	2.654	------
Absorption	**(ASTM C128, 2007)**	0.5%	------
SO_3	**(Iraqi Reference Guide No. 500, 1994)**	0.05%	≤0.1%
Dry rodded density	**(ASTM C29, 2007)**	1645 kg/m^3	------

2.1.4 Silica Fume (SF)

Actually, silica fume, condensed silica fume, often referred to as micro silica, is a pozzolanic material. In this study, silica fume was used to replace 10% of the cement's weight. According

to the results, silica fume conforms with **(ASTM C1240, 2015)**. The chemical and physical properties of silica fume are presented in **Tables 7 and 8**.

Table 7. Physical properties of silica fume.

Property	Test result	(ASTM C1240, 2015)
retained on 45-µm (No. 325) sieve, %	7.5	≤ 10
Accelerated pozzolanic Strength activity index @ 7 days, %	119	≥ 105
Specific surface area, m^2/g	17	≥ 15

Table 8. Chemical analysis of silica fume.

Oxide composition	Oxide content %	(ASTM C1240, 2015)
SiO_2	90.4	≥ 85.0
L.O. I	2.8	≤ 6.0
Moisture content	0.38	≤ 3.0

2.1.5 Chemical Admixture (Super-Plasticizer)

In this investigation, the super-plasticizer (SP) with a dose range of (0.15-1) liter was added for every 100 kg of cementitious materials. It is used to achieve high early strength, high flow ability, and low water content. It satisfies (**ASTM C494, 2013)**, type F, and it does not contain chlorides. **Table 9** illustrates this admixture's characteristics.

Table 9. Technical properties of super-plasticizer (given by manufacturer).

Appearance	**Transparent or Light Brown Liquid**
Calcium Chloride	Nil
Density	1.10 ± 0.02 gm/ml
Viscosity	450 cPs @ 20°C
Setting time	Initial and final setting time depends on temperature, cement quantity, and dosage used.

2.1.6 Water

Water was used in this experiment for the mixing and curing of the concrete mixtures. Moreover, it conforms to Iraqi specifications. **(IQS No. 1703, 2018)**.

2.1.7 perlite

Lightweight expanded perlite, as seen in **Fig. 1**, is used in this investigation. A portion of the coarse aggregate was replaced with perlite, which has a bulk density of 145 kg/m^3 and an S.G. of 0.40. **Table 10** displays the perlite distributions.

Table 10. Grading of Perlite as Partial Replacement of Coarse Aggregate.

Sieve size (mm)	Passing %	(ASTM C330, 2017) Nominal size 2.36-9.5 mm
12.5	100	100
9.5	100	80 - 100
4.75	35	5 - 40
2.36	10	0-20

Figure 1. Image of perlite aggregate

2.2 SCC Mixes

According to **(EFNARC, 2005)**, multiple trail mixes had been carried out. In this experiment, one combination was selected as the control mix, and four groups of SCC mixes—0% perlite, 20% perlite, 40% perlite, and 50% perlite—were tested utilizing perlite volume friction. Al Sarraf **(Al Sarraf et al., 2013)** provided a description of the mixing technique employed in this investigation. **Table 11** displays the specific concrete mixes, with R denoting the reference mix, PG denoting SCC mixes partially replaced with perlite material in place of coarse aggregate, and PS denoting SCC mixes partially replaced with perlite material in place of fine aggregate.

Table 11. Details of Mix design for Self-Compacting Concrete Mixes.

Mixes	Cement kg/m³	Silica fume kg/m³	Coarse aggregate kg/m³	Water kg/m³	w/p	Sand kg/m³	perlite kg/m³	%SP by wt. of cementitious materials
R	540	54	750	188	0.32	865.8	0	1
PG20%	540	54	736.97	188	0.32	865.8	13.03	1
PG40%	540	54	723.96	188	0.32	865.8	26.04	1
PG50%	540	54	717.45	188	0.32	865.8	32.55	1

2.3 Specimen Preparation, Casting, and Curing

When the mixing process was finished, the steel molds were prepared, cleaned, and oil-lubricated before the concrete was poured into them without the need for vibration. The specimens were then covered with nylon sheets. After twenty-four hours, the molds were taken out of the casts. After that, the specimens were taken out of the tanks and allowed to be cured for a further 28 days in the laboratory. In the meantime, the samples were cured in a water tank.

2.4 Testing Program

2.4.1 Fresh Properties Tests of PSCC

Five tests were conducted to analyze the novel qualities of PSCC: the sieve segregation test evaluated resistance to segregation, the slump flow test evaluated flowability, the T500mm and V- funnel tests evaluated viscosity and flowability, and the L-box test evaluated passing ability. **(EFNARC, 2005)** was followed in the running of these tests.

2.4.2 Harden Properties Tests of (PSCC)

2.4.2.1 Compressive Strength Test

According to **(BS EN 12390-3, 2019)**, a cube with dimensions of (10×10×10) cm was used to conduct the compressive strength test for each mix. For this test, a hydromechanical test apparatus with a 2000 KN capacity and a 2.5 MPa/s loading rate was employed. In this study, cubes ages 7, 28, and 56 days were employed. The three specimens at each age were averaged to estimate the compressive strength. Each cube's compressive strength has been calculated using Eq. (1).

$$f_c = F/A_c \quad (1)$$

Where:
f_c = compressive strength, MPa
F = maximum applied load, N
A_c = sample surface area, mm^2

2.4.2.2 Splitting Tensile Strength Test

Cylinder specimens of 100 mm in diameter and 200 mm in height were utilized for the splitting tensile strength test following **(ASTM C496/C496M, 2017)**. The splitting tensile strength of cylinders was measured using a hydromechanical test device. The test included specimens that were 7, 28, and 56 days old. The three specimens at each age were averaged to determine the splitting tensile strength. The splitting strength of concrete specimens was calculated using Eq. (2).

$$T = 2P / \pi ld \quad (2)$$

Where:
T = splitting tensile strength, MPa
P = maximum applied load, N
d = cylinder diameter, (mm)
l = cylinder length, (mm)

2.4.2.3 Flexural Strength Test

As per (**ASTM C293/C293M, 2016)**, the flexural strength was evaluated on prism specimens of 80x80x380 mm, which were supported simply under center point force. The ages of the specimens employed in this research were 7, 28, and 56 days. By averaging the three specimens at each age, the flexural strength was found. The flexural strength of the sample was calculated using Eq. (3).

$$R = 3\,PL/2bd^2 \quad (3)$$

Where:
R = flexural strength, MPa

P = maximum applied load, N
L = span length, mm
b = specimen width, mm
d = specimen depth, mm

2.5 Burning Procedure and Cooling Methods

After 28 days, all samples were removed from the tank and kept in the lab for a further 28 days, following **(Salih and Jasim, 2009)**. As seen in **Fig. 2**, the specimens were burned in a furnace measuring 3500 x 2000 x 900 mm. As seen in **Fig. 3**, a digital thermometer was used to determine the burning temperature. Three different burning temperatures (300, 500, and 700 ˚C) were applied to the specimens. By increasing the exposure rate following the fire curve shown in **Figs.4 and 5** defined in **(ASTM E119-00a, 2017)**, each burning temperature was attained. The cooled furnace was filled with the specimens. Comparable to previous studies by **(Salih and Jasim, 2009; Al-Radi et al., 2021)** the specimens were maintained at the target burning temperature for an hour after it was reached. Before being analyzed, half of the specimens were removed from the furnace and allowed to cool to laboratory temperatures, whereas the other half were subjected to a quick cooling process by being submerged in water tanks.

Figure.2 Burning furnace

Figure.3 Digital thermometer

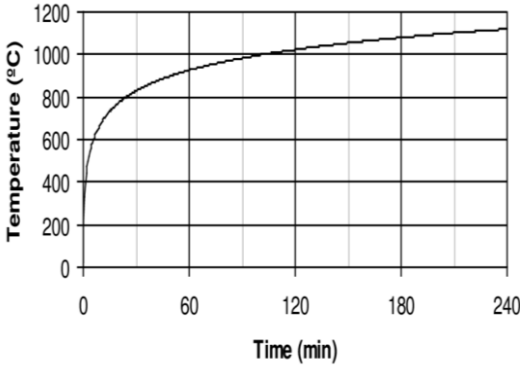

Figure. 4 Fire Curve **(ASTM E119-00a, 2017)**

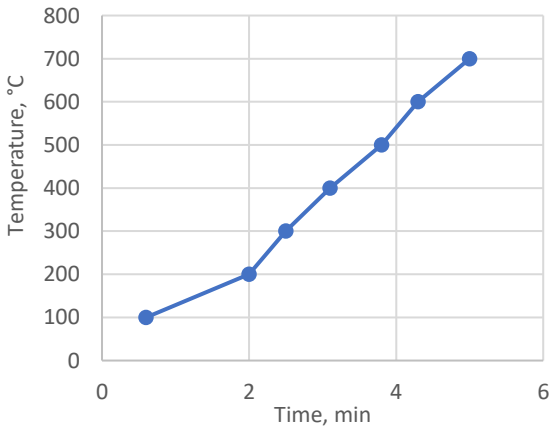

Figure. 5 The fire Curve was relied based on **(ASTM E119-00a, 2017)**

3. RESULTS AND DISCUSSION

3.1 Fresh Properties

Table 12 presents the results of the tests conducted on freshly mixed concrete, as illustrated in **Fig. 6** slump flow test, **Fig. 7. Fig.8** displays the L-box test and illustrates the V-box test. These tests consist of sieve segregation, slump flow, T500mm, V-funnel, and L-box. The workability decreased as the percentage of perlite increased by 0, 20, 40%, and 50%, according to the data. But the fall was reduced to 8% when perlite took the place of half of the coarse aggregate. Perlite in the concrete mix absorbed water, reducing SCC flowability and contributing to the lowering of slump flow **(Türkmen and Kantarci, 2007)**. Using the Segregation Index, the resistance of self-compacting concrete to segregation is measured. According to EFNARC guidelines, results obtained for all mixes within the range of 10.4% to 14.9% have been considered acceptable (<15%) for self-compacting concrete. This shows that all mixes are in compliance with **(Mansour, 2020)** and are classified as SR2.

Table 12. Fresh properties of PSCC mixes.

mix	Slump (mm)	T_{500} (sec)	V-funnel (sec)	L-box	SI %
R	715	2.9	9	0.89	14.9
PG20%	700	3.5	10.1	0.86	14.1
PG40%	680	4	11.5	0.83	12
PG50%	662	4.5	12	0.82	10.8
Limits of (EFNARC, 2005)	SF1 550-650 SF2 660-750 SF3 760-850	VS1/VF1≤ 2 VS2/VF2 >2	≤ 8 9 to 25	>0.80	SR1 ≤ 20 SR2 ≤ 15

Figure. 6 Slump flow test

Figure. 7 V-funnel test

Figure. 8 L-box test

3.2 Compressive Strength

Compressive strength is one of the most crucial characteristics of concrete when it has been set. Results for compressive strength 56 days before and following burning are shown in **Table 13** and **Fig.9**. The results show that the procedure of continuous hydration produces a new hydration product, which accounts for the strength of the concrete at 56 days **(Howlader et al., 2012).** The compressive strength of every concrete sample decreased as the percentage of perlite components rose. It was demonstrated that compressive strength values decreased with increasing perlite ratios. The weak and porous structures of perlite were the reason for this. This can be explained by the porous perlite being used in place of the standard aggregate; the reduced strength and specific gravity (SG = 0.40) of the perlite caused a further decrease in the compressive strength of the concrete **(Oktay et al., 2015)**.

Table 13. Compressive Strength test results after burning.

Mix	Compressive strength MPa at 56 days before burning	compressive strength (MPa) after burning					
		300 °C		500 °C		700 °C	
		Sudden cooling	Gradual cooling	Sudden cooling	Gradual cooling	Sudden cooling	Gradual cooling
R	45	33	35	24	25	13.7	15.3
PG20%	39.1	30.3	31.5	22	23	12.3	14
PG40%	28.5	24.2	24.8	17.1	18.1	11	11.9
PG50%	27.3	23.7	24.5	16.6	17.8	10.7	11.7

Figure 9. Compressive strength Test.

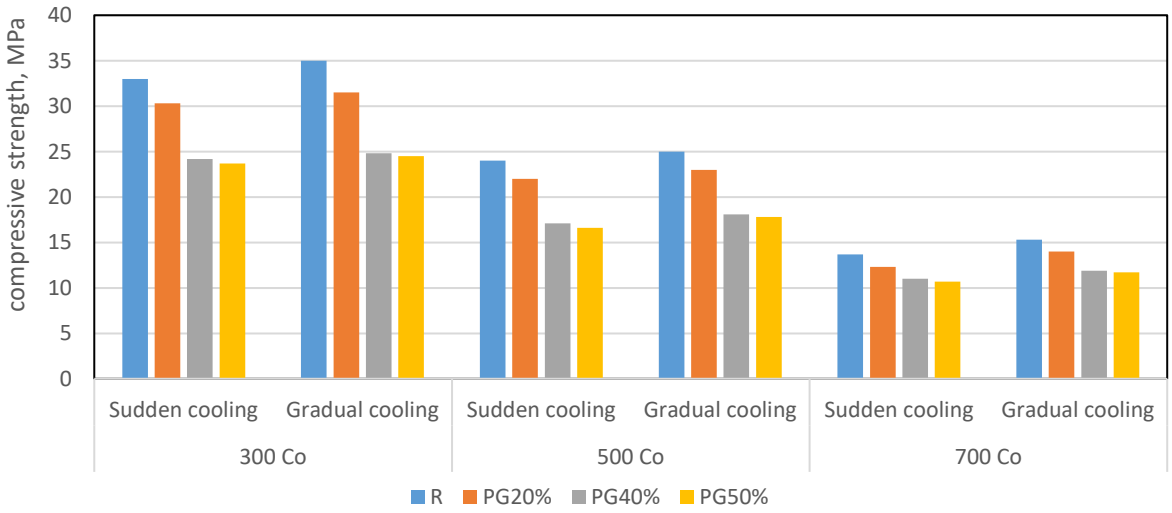

Figure 10. Impact of perlite partial replacement of coarse aggregate on compressive strength after burning

The residual compressive strength of each specimen at 56 days following the burning process is displayed in **Table 14** and **Fig. 11**. The proportion of residual compressive strength that is computed for every outcome following burning in comparison to the identical outcome just before burning Compared to the 50% perlite mixture before burning, the mixes with 50% perlite replacement was the least affected by heat rising and had the highest residual compressive strength. This is due to the increase of internal voids with the increase of perlite replacement, which gives more flexibility to moisture movement and minimizes the stresses inside. It is also evident that the compressive strength significantly decreased as the burning temperature rose by (300, 500, and 700) °C

Table 14. Results of percentage residual compressive strength after burning.

Mix	Residual percentage of compressive strength					
	300 °C		500 °C		700 °C	
	Sudden cooling	Gradual cooling	Sudden cooling	Gradual cooling	Sudden cooling	Gradual cooling
R	73.4	77.78	53.34	55.56	30.45	34
PG20%	77.5	80.57	56.27	58.83	31.46	35.81
PG40%	84.92	87.02	60	63.51	38.6	41.76
PG50%	86.82	89.75	60.81	65.21	39.2	42.86

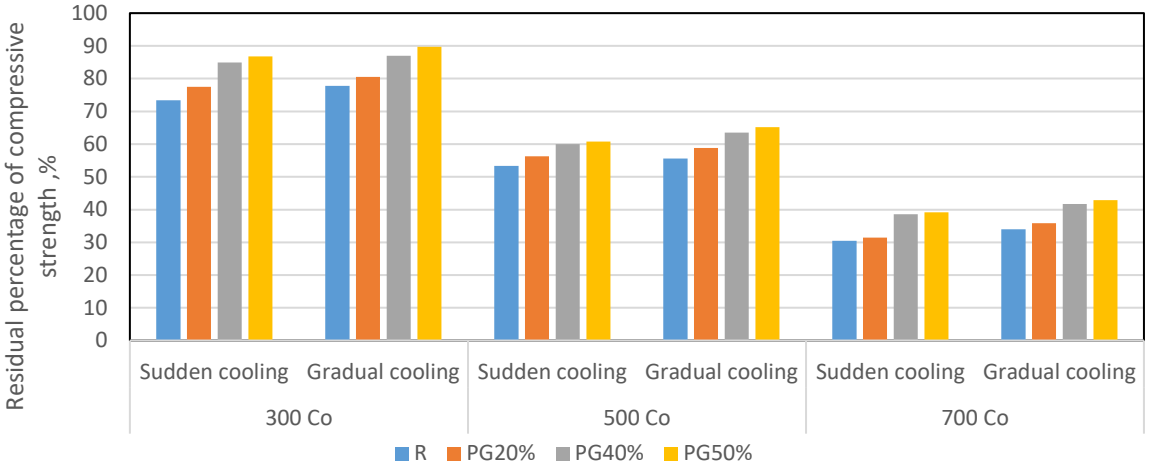

Figure 11. Percentage residual compressive strength after burning

3.3 Flexural Strength

The flexural strength results for each SCC 56 days after burning the mixes used in this study are displayed in **Table 15** and **Fig. 12**. The flexural strength test behavior is depicted in **Fig. 13**. When PG 50% was gradually cooled, the reduction ratios for its flexural strength at age 56 days compared to the Reference mix specimen were 35.29%. **Fig.14** and **Table 16** show the residual percentage of flexural strength after burning. Sudden cooling gave results lower than gradual cooling for the same mix. Whenever the burning temperature increases the difference between the results of sudden and gradual cooling increases.

Table 15. Findings of Flexural Strength test after burning.

Mix	Flexural strength MPa at 56 days before burning	Flexural strength (MPa) after burning					
		300 °C		500 °C		700 °C	
		Sudden cooling	Gradual cooling	Sudden cooling	Gradual cooling	Sudden cooling	Gradual cooling
R	7.1	3.7	3.9	2.2	2.8	1.8	2.18
PG20%	6.2	4.1	4.4	2.7	2.9	2.2	2.58
PG40%	5.6	4.6	4.8	3	3.2	2.6	2.9
PG50%	5.1	4.7	4.85	3.4	3.6	2.8	3.3

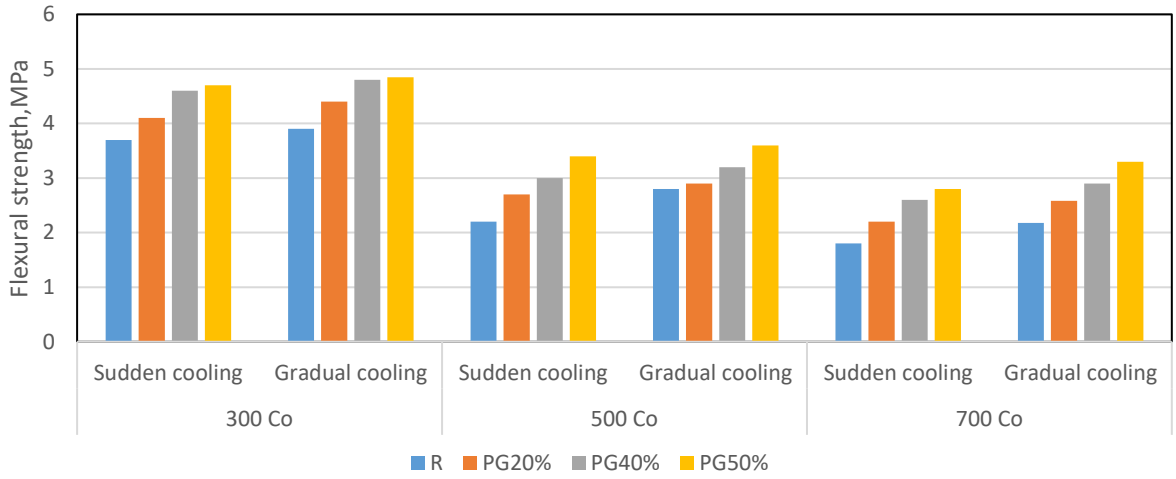

Figure 12. Effect of perlite replacement of coarse aggregate on flexural strength after burning

Figure 13. Flexural strength test

Table 16. Results of percentage residual flexural strength after burning.

Mix	Residual percentage of Flexural strength					
	300 °C		500 °C		700 °C	
	Sudden cooling	Gradual cooling	Sudden cooling	Gradual cooling	Sudden cooling	Gradual cooling
R	52.12	54.93	30.99	39.44	25.36	30.71
PG20%	66.13	70.97	43.55	46.78	35.49	41.62
PG40%	82.15	85.72	53.58	57.15	46.43	51.79
PG50%	92.16	95.1	66.67	70.59	54.91	64.71

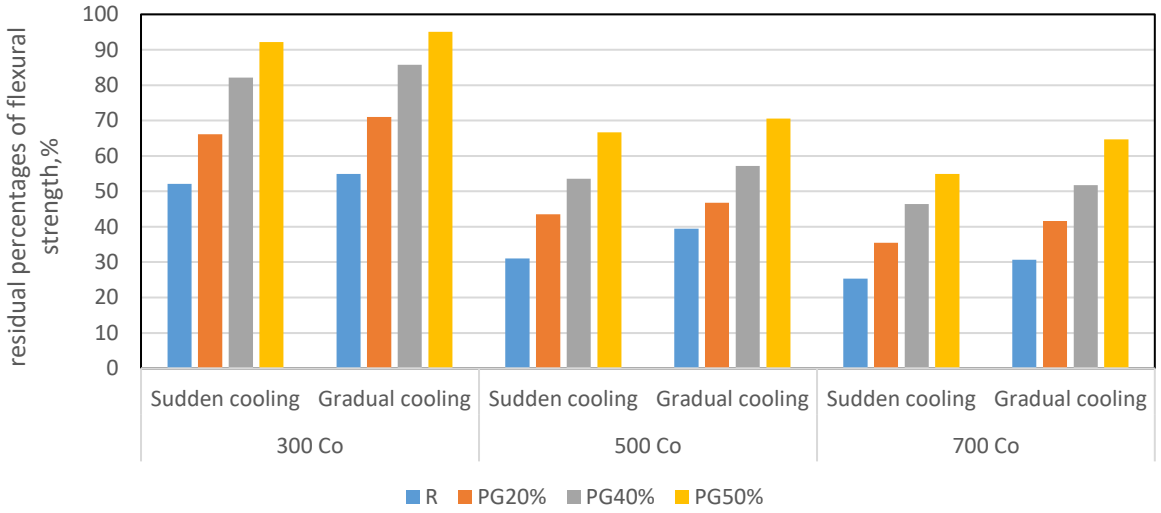

Figure 14. Percentage residual flexural strength after burning

3.4 Splitting Tensile Strength

It's obvious from **Table 17, Fig. 15**, which shows the splitting test results before and after burning at a 56-day age, that the addition of lightweight aggregate has reduced this type of strength. When PG 50% was cooled gradually, the reduction ratios for the splitting strength were 48.69% when compared to the reference mix specimen at 56 days of age. Splitting tensile test results are displayed in **Fig. 16**. The results of percentages of residual splitting tensile strength are displayed in **Table 18** and **Fig. 17.** The reason for the marginal increase in splitting tensile strength following burning is related to the low thermal conductivity of perlite, which means that as perlite content rises, so do the gaps within the mixes, resulting in a decrease in thermal conductivity and a reduction in the burning effect **(Tandiroglu, 2010)**.

Table 17. Splitting Tensile strength test results after burning.

Mix	Splitting tensile strength MPa at 56 days before burning	Splitting tensile strength (MPa) after burning					
		300 °C		500 °C		700 °C	
		Sudden cooling	Gradual cooling	Sudden cooling	Gradual cooling	Sudden cooling	Gradual cooling
R	5.01	3	3.17	1.90	1.94	0.94	1.18
PG20%	4.11	3.24	3.3	1.98	2.08	1.22	1.49
PG40%	3.62	3.26	3.39	2.26	2.41	1.31	1.54
PG50%	3.45	3.30	3.41	2.88	2.94	1.52	1.77

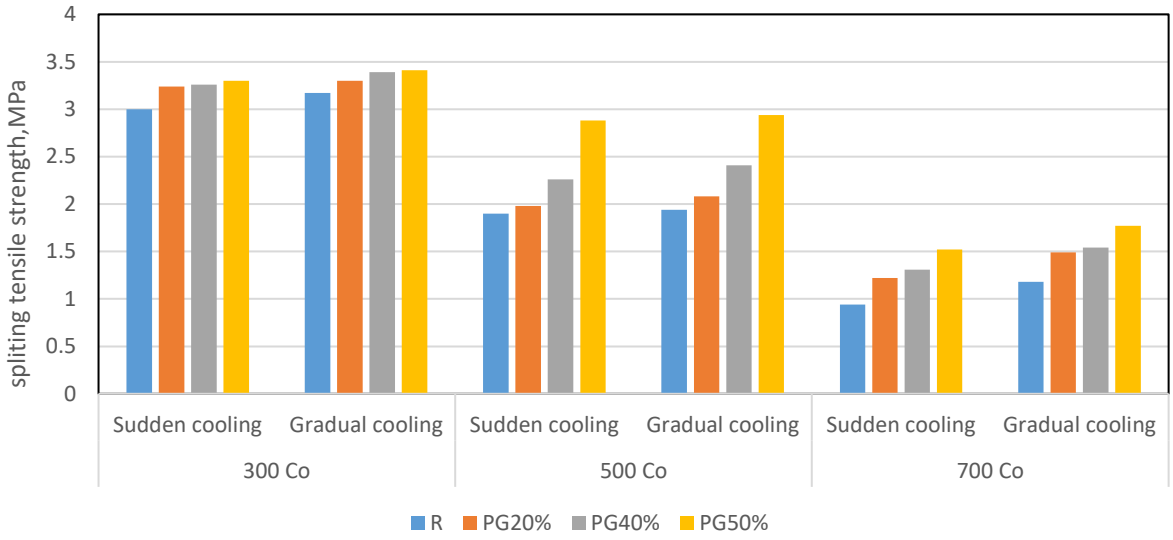

Figure 15. Effect of perlite replacement of coarse aggregate on splitting tensile strength after burning

Figure 16. Splitting tensile strength test

Table 18. Results of percentage residual splitting tensile strength after burning.

Mix	Residual percentage of Spiting tensile strength					
	300 °C		500 °C		700 °C	
	Sudden cooling	Gradual cooling	Sudden cooling	Gradual cooling	Sudden cooling	Gradual cooling
R	59.89	63.28	37.93	38.73	18.77	23.56
PG20%	78.84	80.3	48.18	50.61	29.69	31.64
PG40%	90.06	93.65	62.44	66.58	36.19	42.55
PG50%	95.66	98.85	83.48	85.22	44.06	51.31

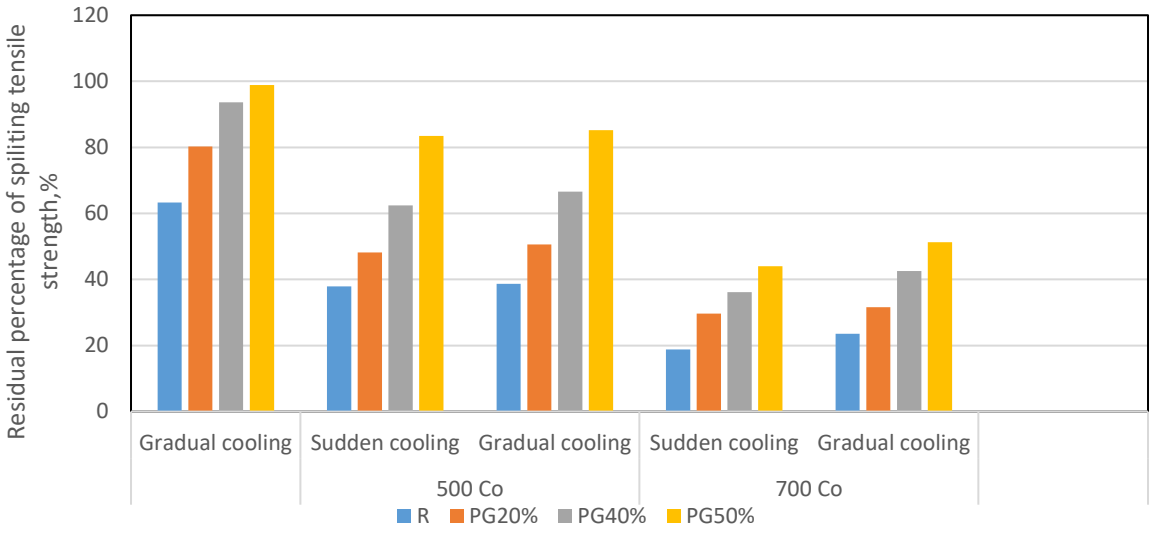

Figure 17. Percentage residual splitting tensile strength after burning

4. CONCLUSIONS

- Gradually, workability was reduced when coarse aggregate was replaced with perlite with percentages (20, 40, and 50%).
- The mechanical properties of all mixtures (compressive, flexural, and splitting tensile strengths) showed a significant decline, reaching their lowest values at a 50% perlite concentration.
- As the temperature at which concrete burns increases, the residual compressive, flexural, and splitting tensile strengths decrease.
- Strength retention following burning increases in line with an increase in perlite replacement.
- Sudden cooling gave results lower than gradual cooling for the same mix. Whenever the burning temperature increases the difference between the results of sudden and gradual cooling increases.
- No spalling was observed at 700C^{o}.

Acknowledgements

This work was supported by the department of Civil Engineering, College of Engineering, University of Baghdad.

Credit Authorship Contribution Statement

Baraa Qays Naeem: Experimental work, writing, and editing.
Hadeel Khalid Awad: Supervision, reviewing, evaluation, and editing.

Declaration of Competing Interest

The authors declare that they have no known competing financial interests or personal relationships that could have appeared to influence the work reported in this paper.

REFERENCES

Al-Daraji, M. and Aljalawi, N., 2024. The effect of kevlar fibers on the mechanical properties of lightweight perlite concrete. *Engineering, Technology & Applied Science Research*, 14(1), pp.12906-12910. https://doi.org/10.48084/etasr.6665.

Aljalawi, N.M. and Ahmad, H.I., 2014. Effect of local feldspar on the properties of self-compacting concrete. *Journal of Engineering*, 20(09), pp.1-13. https://dx.doi.org/10.1088/1755-1315/1374/1/012013.

Al-Kabi, W.H. and Awad, H.K., 2024. Investigating some properties of hybrid fiber reinforced LECA lightweight self-compacting concrete. *Journal of Engineering*, 30(03), pp.177-190. https://doi.org/10.31026/j.eng.2024.03.12.

Al-Obaidy, H.K.A., 2017. Influence of internal Sulfate attack on some properties of self-compacted concrete. *Journal of Engineering*, 23(5), pp.27-46. https://doi.org/10.31026/j.eng.2024.12.09.

AL-Radi, H.Y., Dejian, S. and Sultan, H.K., 2021. Performance of fiber self-compacting concrete at high temperatures. *Civil Engineering Journal*, 7(12), pp.2083-2098. https://dx.doi.org/10.28991/cej-2021-03091779.

Alsaedy, S.M. and Aljalawi, N., 2021. The effect of nanomaterials on the properties of limestone dust green concrete. *Engineering, Technology & Applied Science Research*, 11(5), pp.7619-7623. https://doi.org/10.48084/etasr.4371.

Al Sarraf, S.Z., Hamoodi, M.J. and Ihsan, M.A., 2013. High strength self-compacted concrete mix design. *International Journal of Civil Engineering*, 2(4), pp.83-92.

Aslani, F. and Kelin, J., 2018. Assessment and development of high-performance fiber-reinforced lightweight self-compacting concrete including recycled crumb rubber aggregates exposed to elevated temperatures. *Journal of cleaner production*, 200, pp.1009-1025. https://doi.org/10.1016/j.jclepro.2018.07.323.

ASTM C330, 2017. Standard Specification for Lightweight Aggregate for Structural Concrete. *American Society for Testing and Material*. 4(2), pp.4. https://doi.10.1520/C0330_C0330M-17A.

ASTM C127, 2007. Standard Test Method for Density, Relative Density (Specific Gravity), and Absorption of Coarse Aggregate. *ASTM International*. 4(2), pp.6. https://doi.10.1520/C0127-24.

ASTM C128, 2007. Standard Test Method for Density, Relative Density (Specific Gravity), and Absorption of Fine Aggregate. *ASTM International*. 4(2), pp.7. http://doi.10.1520/C0128-07.

ASTM C29, 2007. Standard Test Method for Bulk Density (Unit Weight) and Voids in Aggregate. *ASTM International*. 4(2),, pp.5. http://doi.10.1520/C0029_C0029M-23.

ASTM C1240, 2015. Standard specification for silica fume used in cementitious mixtures. *ASTM International*. 4(2),, pp.7. http://doi.10.1520/C1240-12.

ASTM C293/C293M, 2016. Standard test method for flexural strength of concrete (using simple beam with center-point loading). ASTM International.

ASTM C494, 2013. Standard specification for chemical admixtures for concrete. American Society for Testing and Material.

ASTM C496/C496M, 2017. Standard Test Method for Splitting Tensile Strength of Cylindrical Concrete Specimens.

ASTM E119-00a , 2017. Standard Test Methods for Fire Tests of Building Construction and Materials.

BS EN 12390-3, 2019. Compressive strength of test specimens. British Standards Institution.

Cojocaru, A., Isopescu, D.N. and Maxineasa, S.G., 2023, June. Perlite concrete: a review. *In IOP Conference Series: Materials Science and Engineering* (Vol. 1283, No. 1, p. 012003). IOP Publishing.

EFNARC, 2005. The European guidelines for self-compacting concrete: Specification, production and use.

Gandage, A.S., Rao, V.V., Sivakumar, M.V.N., Vasan, A., Venu, M. and Yaswanth, A.B., 2013. Effect of perlite on thermal conductivity of self-compacting concrete. *Procedia-Social and Behavioral Sciences*, 104, pp.188-197. https://doi.org/10.1016/j.sbspro.2013.11.111.

Howlader, M.K., Rashid, M.H., Mallick, D. and Haque, T., 2012. Effects of aggregate types on thermal properties of concrete. *ARPN Journal of Engineering and Applied Sciences*, 7(7), pp.900-906.

Hubertova, M., 2005. Self-compacting light concrete with liapor aggregates. *In Young Researchers' Forum: Proceedings of the International Conference held at the University of Dundee, Scotland*, UK on 7 July 2005 (pp. 103-112). Thomas Telford Publishing.

IQS, No. 5., 2019. Portland Cement. Central Organization for Standardization and Quality Control. Iraqi Specification.

IQS, No.1703., 2018. used water in concrete. Iraqi Specification.

Iraqi Reference Guide No. 500, 1994. Sulfate Content Test of Aggregate. Central Organization for Standardization and Quality Control, Baghdad.

Jedidi, M., Benjeddou, O. and Soussi, C., 2015. Effect of expanded perlite aggregate dosage on properties of lightweight concrete. *Jordan Journal of Civil Engineering*, 9(3).

Mansour, S.M., 2020. Behavior of self-compacting concrete incorporating calcined pyrophyllite as supplementary cementitious material. *Journal of Building Materials and Structures*, 7(1), pp.119-129. https://doi.org/10.34118/jbms.v7i1.744.

Mladenovič, A., Šuput, J.S., Ducman, V. and Škapin, A.S., 2004. Alkali–silica reactivity of some frequently used lightweight aggregates. *Cement and concrete research*, 34(10), pp.1809-1816. https://doi.org/10.1016/j.cemconres.2004.01.017.

Oktay, H., Yumrutaş, R. and Akpolat, A., 2015. Mechanical and thermophysical properties of lightweight aggregate concretes. *Construction and Building Materials*, 96, pp.217-225. https://doi.org/10.1016/j.conbuildmat.2015.08.015.

Premalatha, P.V., Geethanjali, M., Rahuraman, T. and Gurusaran, S., 2023. Experimental study on concrete behaviour with partial replacement of M-Sand with unexpanded perlite. *In E3S Web of Conferences* (Vol. 405, p. 03020). *EDP Sciences*. https://doi.org/10.1051/e3sconf /202340503020.

Rashad, A.M., 2016. A synopsis about perlite as building material–A best practice guide for Civil Engineer. *Construction and Building Materials*, 121, pp.338-353. https://doi.org/10.1016/j.conbuildmat.2016.06.001.

Salih, S.A. and Jasim, A.T., 2009. Performance of fiber lightweight aggregate concrete exposed to elevated temperatures. *Engineering &Technology*, 27, p.13.

Sengul, O., Azizi, S., Karaosmanoglu, F. and Tasdemir, M.A., 2011. Effect of expanded perlite on the mechanical properties and thermal conductivity of lightweight concrete. *Energy and Buildings*, 43(2-3), pp.671-676. https://doi.org/10.1016/j.enbuild.2010.11.008.

Shamran, A.S. and Abbas, Z.K., 2024. Fabricating a sustainable roller compacted concrete containing recycled waste demolished materials: A literature review. *Journal of Engineering*, *30*(03), pp.15-29. https://doi.org/10.31026/j.eng.2024.03.02.

Sodeyama, K., Sakka, Y., Kamino, Y. and Seki, H., 1999. Preparation of fine expanded perlite. *Journal of Materials Science, 34, pp.2461-2468*. https://doi.org/10.1023/A:1004579120164.

Tandiroglu, A., 2010. Temperature-dependent thermal conductivity of high-strength lightweight raw perlite aggregate concrete. *International journal of thermophysics*, 31, pp.1195-1211. https://doi.org/10.1007/s10765-010-0826-5.

Türkmen, İ. and Kantarcı, A., 2006. Effects of expanded perlite aggregate and different curing conditions on the drying shrinkage of self-compacting concrete. *Indian Journal of Engineering & Materials Sciences*, 13(3), pp.247-252.

Türkmen, İ. and Kantarcı, A., 2007. Effects of expanded perlite aggregate and different curing conditions on the physical and mechanical properties of self-compacting concrete. *Building and Environment*, 42(6), pp.2378-2383. https://doi.org/10.1016/j.buildenv.2006.06.002.

تأثير استبدال ركام البيرلايت جزئيا بالركام الخشن على سلوك خرسانة ذاتية الرص والمعرضة للهب النار مع استخدام طرق تبريد مختلفة

براء قيس نعيم* ، هديل خالد عواد

قسم الهندسة المدنية، كلية الهندسة، جامعة بغداد، بغداد، العراق

الخلاصة

تهدف هذه الدراسة إلى تقييم خواص الخرسانة ذاتية الرص في حالتها الطرية والمتصلبة والتي استخدم فيها ركام البيرلايت المستبدل جزئيا من الركام الخشن. تم في هذه الدراسة استخدام 594 كغم/م^3 من مادة رابطة في خلطة خرسانية ذاتية الرص. تم إجراء أربع خلطات خرسانية باستخدام البيرلايت كبديل جزئي للركام الخشن بنسب حجمية (0، 20، 40، 50) %. تم اختبار خصائص الخرسانة الطازجة باستخدام اختبارات (التدفق، القمع على شكل حرف V، الصندوق على شكل حرف L، ومؤشر العزل). يتم اختبار الخرسانة المتصلبة بعمر 56 يوما بعد عملية حرقها. تقيس هذه الاختبارات قوة الضغط والانقسام والانحناء. أظهرت النتائج أن محتوى البيرلايت يقلل من قابلية التشغيل. تنخفض مقاومة الانضغاط والانثناء والشد بشكل ملحوظ مقارنة بالخليط المرجعي مع زيادة نسبة البيرلايت. بعد حرقها عند درجات حرارة (300، 500، 700) درجة سيليزية، تم تبريد نصف العينات تدريجياً قبل اختبارها، وتم تبريد النصف الآخر من العينات فجأة باستخدام خزانات المياه. قل مقدار النقصان في مقاومة الانضغاط بعد الاحتراق مع زيادة استبدال البيرلايت في الخليط. وكانت النسب المتبقية لمقاومة الانضغاط عند 56 يوما بعد الحرق هي الأعلى عند 50% بيرلايت، مع (65.21،89.75 و42.86) % عند 300، 500، 700 درجة سيليزية على التوالي للتبريد التدريجي. وكانت النسب المتبقية لمقاومة الشد الانشطاري عند 56 يوما بعد الحرق لنماذج الخرسانة ذاتيه الرص الحاوية على بيرلايت مستبدل بنسبة 50% من الركام الخشن هي (85.22،98.85، 51.31) % عند 300، 500، 700 درجة سيليزية على التوالي للتبريد التدريجي.

الكلمات المفتاحية: الركام الخشن، لهب النار، ركام البيرلايت، خرسانة ذاتية الرص.